



King Saud University  
Arabian Journal of Chemistry

www.ksu.edu.sa  
www.sciencedirect.com



## ORIGINAL ARTICLE

# Physicochemical properties, antioxidant action and practical application in fresh cheese of the solid inclusion compound $\gamma$ -cyclodextrin-quercetin, in comparison with $\beta$ -cyclodextrin-quercetin

Ana Bárbara Pereira<sup>a</sup>, Aida Moreira da Silva<sup>b,c</sup>, Maria João Barroca<sup>b</sup>,  
Maria Paula M. Marques<sup>b,d</sup>, Susana Santos Braga<sup>a,\*</sup>

<sup>a</sup> QOPNA, Department of Chemistry, University of Aveiro, 3810-193 Aveiro, Portugal

<sup>b</sup> R&D Group "Molecular Physical-Chemistry – QFM-UC", University of Coimbra, 3004-535 Coimbra, Portugal

<sup>c</sup> Department of Food Science and Technology, ESAC-IPC, Bencanta, 3040-316 Coimbra, Portugal

<sup>d</sup> Dep. Life Sciences, Univ. Coimbra, 3000-456 Coimbra, Portugal

Received 14 October 2016; accepted 1 April 2017

## CHEMICAL COMPOUNDS STUDIED IN THIS ARTICLE

Quercetin (PubChem: CID5280343);  
 $\beta$ -cyclodextrin (PubChem: CID444041);  
 $\gamma$ -cyclodextrin (PubChem: CID86575)

## KEYWORDS

Quercetin;  
Cyclodextrin inclusion;  
Antioxidant;  
Fresh cheese;  
Sensorial evaluation

**Abstract** Quercetin is an antioxidant flavonol very sensible to light and oxidants that can benefit from stabilisation by encapsulation into cyclodextrins. In this work we study the solid inclusion compounds of quercetin with  $\beta$ - and  $\gamma$ -cyclodextrins ( $\beta$ -CD and  $\gamma$ -CD) obtained by freeze-drying. Combined results from microanalysis, FT-IR, powder X-ray diffraction,  $^{13}\text{C}\{^1\text{H}\}$  CP/MAS NMR spectroscopy and thermogravimetry demonstrating that  $\gamma$ -CD, having a larger cavity, is the most adequate host to form a stable inclusion complex with quercetin. The anti-peroxidation capacity of the compounds was determined and followed the order  $\beta$ -CD-quercetin  $\gg$  quercetin  $>$   $\gamma$ -CD-quercetin. Both  $\gamma$ -CD-quercetin and  $\beta$ -CD-quercetin are able to inhibit DPPH radicals at a rate three times faster than pure quercetin, but their  $\text{EC}_{50}$  is higher (50  $\mu\text{M}$  vs 17  $\mu\text{M}$  for quercetin). The practical applicability of the two CD-quercetin adducts as nutraceutical additives in fresh cheese was established. Fortified fresh cheese had a firmer texture and yellowish colour, but no significant changes in the overall sensorial qualities were found by a panel of non-trained tasters when compared with the control (non-treated fresh cheese).

© 2017 The Authors. Production and hosting by Elsevier B.V. on behalf of King Saud University. This is an open access article under the CC BY-NC-ND license (<http://creativecommons.org/licenses/by-nc-nd/4.0/>).

\* Corresponding author.

E-mail address: [sbraga@ua.pt](mailto:sbraga@ua.pt) (S.S. Braga).

Peer review under responsibility of King Saud University.



Production and hosting by Elsevier

## 1. Introduction

A growing topic in food research is the fortification of food with nutraceuticals or other health promoting ingredients, such as probiotics or vitamins, to obtain functional foods. Flavonoids, for their antioxidant properties, are among the most widely used phytochemicals, appearing in cookies (Paul and Bhattacharyya, 2015) and a

<http://dx.doi.org/10.1016/j.arabjc.2017.04.001>

1878-5352 © 2017 The Authors. Production and hosting by Elsevier B.V. on behalf of King Saud University.

This is an open access article under the CC BY-NC-ND license (<http://creativecommons.org/licenses/by-nc-nd/4.0/>).

Please cite this article in press as: Pereira, A.B. et al., Physicochemical properties, antioxidant action and practical application in fresh cheese of the solid inclusion compound  $\gamma$ -cyclodextrin-quercetin, in comparison with  $\beta$ -cyclodextrin-quercetin. Arabian Journal of Chemistry (2017), <http://dx.doi.org/10.1016/j.arabjc.2017.04.001>

variety of beverages (Rothe et al., 2015; Lanilai.com, 2016; Yehuda and Anglea, 2010). Quercetin is a well-established nutraceutical, particularly suited for food fortification since it allows obtaining products with superior antioxidant and medicinal properties (Boots et al., 2008). Quercetin has a ubiquitous and high-quantity presence in natural sources, which makes it easy to obtain, and it offers the effective antioxidant action within the family of flavonols due to its singular chemical structure. Quercetin occurs in fruits such as cowberries, lingonberries, blueberries, vegetables such as red onions and peppers (chilli or sweet), herbs such as levesticum, dill and tarragon and even in green tea and cocoa (Kozłowska and Szostak-Węgierek, 2014; Quercetin.com, 2016; Stobiecki and Kachlicki, 2006). Chemically, quercetin features a catechol B-ring and three additional hydroxyls on carbons 3, 5 and 7 (Fig. 1a). It is the third most active flavonoid, following epicatechin gallate and epigallocatechin galate (Thilakarathna and Rupasinghe, 2013). Quercetin has a relatively low bioavailability from oral ingestion (Hollman et al., 1996), which varies strongly with the food source and with the degree of cooking (Hollman et al., 1997a, 1997b), but it remains in the plasma for a few days, which allows bioaccumulation from repeated ingestion. It is proposed to act as cardiovascular protecting agent (Hollman et al., 1997a) and other medicinal properties are under study, namely leishmanicidal activity (Sen et al., 2008) and antitumor action against PC-3 prostate cancer cells (Senthilkumar et al., 2010). The absorption, gastrointestinal stability and bioavailability of quercetin can be improved by encapsulation techniques, namely with liposomes (Rasaie et al., 2014) and cyclodextrins (CDs), cyclic oligosaccharides of six to eight 1,4-linked  $\alpha$ -D-glucose units ( $\alpha$ -CD,  $\beta$ -CD and  $\gamma$ -CD) obtained by enzymatic fermentation of starch. By inclusion of hydrophobic compounds into their ring cavities, CDs act not only as solubilisers but also as molecular capsules with protective action against oxidation, hydrolysis and degradation by UV radiation or heat (Pereira and Braga, 2015). Native cyclodextrins are in the spotlight for food modification technologies as a result of their GRAS status ('generally recognised as safe') awarded by the FDA and the WHO-FAO joint committee. They are very useful in increasing the stability of antioxidant molecules, namely  $\alpha$ -tocopherol (Koontz et al., 2009), polyphenols such as rutin, phloridzin and chlorogenic acid (Ramírez-Ambrosi et al., 2014) and, of course, quercetin. Cyclodextrin inclusion of quercetin was previously observed in the solution state (Bergonzi et al., 2007). When  $\beta$ -CD is used, the solubility of quercetin in water was demonstrated to increase by roughly 10-fold (Pralhad and Rajendrakumar, 2004). In turn, in phosphate buffer with 20% DMSO, quercetin interacts faintly with  $\beta$ -CD and small shifts in the  $^1\text{H}$  NMR

signals of quercetin protons at the positions 8, 2' and 6', meaning that the inclusion may occur at one of the two terminal rings of quercetin (ring A or ring C). Furthermore, a preferential 1:1 inclusion stoichiometry was determined (Zheng et al., 2004).

The present work deals with the preparation and characterisation of a solid inclusion compound of  $\gamma$ -CD with quercetin. In addition,  $\beta$ -CD-quercetin in the solid-state was also prepared. This inclusion compound was previously isolated as an amorphous solid, which did not allow a detailed solid-state structural characterisation (Pralhad and Rajendrakumar, 2004). In the present report, it is observed the behaviour of  $\beta$ -CD-quercetin upon recrystallisation and the geometries of inclusion are postulated for both  $\beta$ -CD-quercetin and  $\gamma$ -CD-quercetin. Furthermore, the effect of the cyclodextrins on the antioxidant activity of quercetin is evaluated for the first time, by means of the DPPH and TBARS assays. The application of the adducts as nutraceuticals in a food matrix was investigated. Fresh cheese was chosen as model food since cheese products are much appreciated foods and therefore excellent candidates to convey nutraceuticals to the consumers. Cyclodextrins are suitable carriers for use in dairy products (Marcolino et al., 2011) and they have been widely used in dairy technology, either to remove cholesterol from milk (Tahir et al., 2013) and from cheese varieties such as gouda, camembert and feta (Bae et al., 2008, 2009; Jung et al., 2013), or as taste-masking agents in goat's cheese and yogurt (Young et al., 2012). In light of the ability of CDs to modify the organoleptic characteristics of cheese, a sensorial evaluation of the fresh cheese fortified with CD-quercetin was conducted.

## 2. Materials and methods

### 2.1. Chemicals

$\beta$ -CD and  $\gamma$ -CD (pharma-grade Cavamax W7 and W8, manufactured by Wacker-Chemie) were kindly donated by Ashland Specialty Ingredients (Düsseldorf, Germany). Quercetin was obtained from Discovery Fine Chemicals (UK), potassium bromide (KBr,  $\geq 99\%$ ), thiobarbituric acid (TBA), 2,2'-azobis-(2-amidinopropane) dihydrochloride (AAPH) and 1,1-diphenyl-2-picrylhydrazyl (DPPH) were from Sigma-Aldrich (Sintra, Portugal) and trichloroacetic acid (TCA) was from Farbwerke Hoechst AG (Frankfurt, Germany). All the solvents were of analytical grade and used as received.

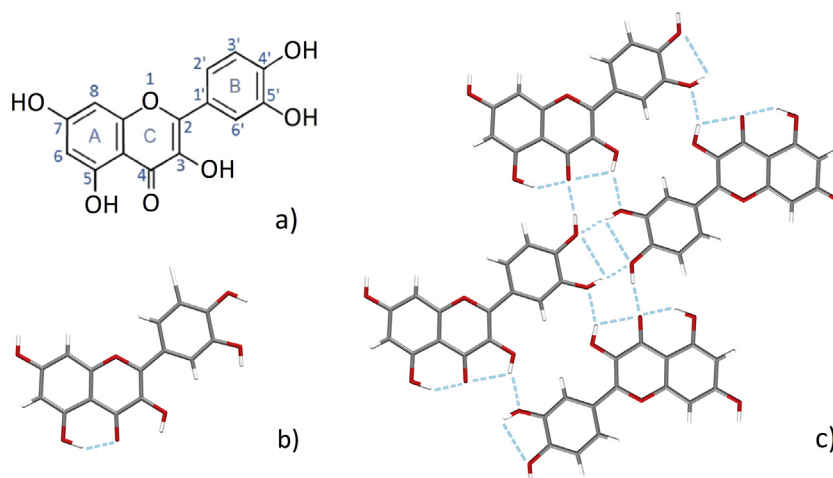


**Figure 1** Quercetin: structure and proposed hydrogen bonds in the solid state. (a) Common labelling used for the aromatic rings of quercetin and its atom numbering scheme; (b) intramolecular hydrogen bond existing in quercetin according to Briggs and Colebrook (1962); (c) intra- and intermolecular hydrogen bonding pattern of quercetin according to Filip et al. (2013).

## 2.2. Equipment

Freeze-drying procedures were carried out in a 1.5 l MicroModulyo Freeze Dryer from Thermo Electron Corporation.

Microanalyses for CHN were performed at the University of Aveiro (Department of Chemistry) on an LECO Elemental Analyser. Samples were combusted under an oxygen atmosphere at 975 °C for 1 min, and helium was used as purge gas.

Powder X-ray diffraction data were collected at ambient temperature on a X'Pert MPD Philips diffractometer (Cu K $\alpha_{1,2}$  X-radiation,  $\lambda_1 = 1.540598 \text{ \AA}$  and  $\lambda_2 = 1.544426 \text{ \AA}$ ), equipped with a X'Celerator detector and a flat-plate sample holder in a Bragg-Brentano para-focusing optics configuration (40 kV, 50 mA). Intensity data were collected by the step-counting method (step 0.02°), in continuous mode, in the ca.  $3.0 \leq 2\theta \leq 50.0^\circ$  range.

SEM images were acquired using a scanning electron microscope Hitachi SU-70 Schottky emission instrument working at 15 kV.

TGA studies were conducted on a Shimadzu TGA-50 system. Samples of mass  $\approx 1\text{--}5$  mg were placed on a 5 mm  $\varnothing$  platinum crucible and heated at 5 °C/min with an air flow of 20 mL/min.

FTIR spectra (range 4000–380  $\text{cm}^{-1}$ ) were collected as KBr pellets using a Unicam Mattson Mod 7000 FTIR spectrophotometer (64 scans, 2  $\text{cm}^{-1}$  resolution); in a typical preparation, 2 mg of sample were mixed in a mortar with 200 mg of KBr.

Raman spectra (range 4000–200  $\text{cm}^{-1}$ ) were acquired at ambient temperature in a Bruker RFS-100 Fourier transform Raman spectrometer with a 180° geometry ( $3 \times 600$  scans, 1  $\text{cm}^{-1}$  resolution), equipped with an InGaAs detector and a Nd:YAG near-infrared excitation laser (1064 nm) by Coherent, model Compass-1064/500 N) yielding 30–50 mW at the sample position.

Solid-state nuclear magnetic resonance spectra with  $^{13}\text{C}$  { $^1\text{H}$ } cross-polarisation and magic angle spinning (CP/MAS NMR) were recorded at 125.72 MHz on a (11.7 T) Bruker Avance 500 spectrometer, with an optimised  $\pi/2$  pulse for  $^1\text{H}$  of 4.5  $\mu\text{s}$ , 2 ms contact time, a spinning rate of 7 kHz and 12 s recycle delays. Chemical shifts are quoted in parts per million from tetramethylsilane.

Absorbance readings for the thiobarbituric acid reactive substances assay (TBARS) assay were collected in a  $\mu\text{Quant}^{\text{TM}}$  Microplate Spectrophotometer from BioTek Instruments, Inc, at a working wavelength of 532 nm.

## 2.3. Preparation of the solid inclusion compounds

### 2.3.1. $\beta$ -CD-Quercetin (1:1)

100 mg (0.076 mmol) of  $\beta$ -CD were dissolved in 10 mL of water at 37 °C. Separately, 23 mg (0.076 mmol) of quercetin were dissolved in 13 mL of ethanol at 37 °C. After full dissolution of both compounds, solutions were mixed, stirred for 3 h and subject to snap freezing (with liquid nitrogen). Solvent removal by freeze-drying afforded a voluminous pale-yellow solid in quasi-quantitative yield.

Anal. Calc. for  $(\text{C}_{42}\text{H}_{70}\text{O}_{35})(\text{C}_{15}\text{H}_{10}\text{O}_7) \cdot 18(\text{H}_2\text{O})$  (1760.6): C, 38.85; H, 6.640%; Found: C, 38.62; H, 6.813%. Thermogravimetric analysis up to 135 °C shows a mass loss of 13.7%, corresponding to the evaporation of 13 water molecules.

FT-IR (KBr,  $\text{cm}^{-1}$ ):  $\nu(\text{tilde}) = 3386\text{vs}$ , 2929m, 1660m, 1612m, 1560m, 1523m, 1450m, 1410m, 1383m, 1324m, 1305sh, 1263m; 1201m, 1157s, 1102sh, 1080s, 1029vs, 1002sh, 947m, 939m, 864m, 843m, 826m, 794w, 756m, 706m, 668w, 656w, 639w, 606m, 578m, 531m, 478w, 445w, 419w, 408w, 400w, 385w, 376w, 359w, 354w, 336w, 328w, 314w, 303w, 297vw, 290w.

Raman:  $\nu(\text{tilde}) = 1660\text{w}$ , 1605vs, 1589m, 1547s, 1439s, 1399m, 1371m, 1327m, 1316m, 1294w, 1267w, 1219w, 1174w, 1112w, 1093vw, 1014vw, 994vw, 942m, 843m, 784m, 721w, 706w, 685 w, 660w, 639m, 603s, 574m, 520m, 478m, 471m, 253w, 231w, 209 vw.

$^{13}\text{C}\{^1\text{H}\}$  CP/MAS NMR: 174.1 (guest,  $\text{C}_4$ ), 163.8 (guest,  $\text{C}_7$ ), 157.2 (guest,  $\text{C}_5$ ), 154.6 (guest,  $\text{C}_9$ ), 147.9 (guest,  $\text{C}_4'$ ), 146.2 (guest,  $\text{C}_2$ ), 141.5 (guest,  $\text{C}_3'$ ), 135.1 (guest,  $\text{C}_3$ ), 125.9 (guest,  $\text{C}_1'$ ), 122.0 (guest,  $\text{C}_6'$ ), 115.5 (guest,  $\text{C}_5'$ ), 112.1 (guest,  $\text{C}_2'$ ), 104.2, 103.3, 102.2, 101.4 (all  $\beta$ -CD,  $\text{C}_1$ ), 95.9 (guest,  $\text{C}_{6,8}$ ), 84.2, 83.3, 82.3, 81.2, 80.4, 78.4 (all  $\beta$ -CD,  $\text{C}_4$ ), 76.3, 75.2, 73.8, 73.0, 72.6, 71.6 (all  $\beta$ -CD,  $\text{C}_{2,3,5}$ ), 63.7, 62.2, 60.3, 59.6, 58.7 (all  $\beta$ -CD,  $\text{C}_6$ ) ppm.

NOTE: For comparison, the  $^{13}\text{C}\{^1\text{H}\}$  CP/MAS NMR spectrum of quercetin was also collected. The resonances of pure quercetin are as follows: 174.4 ( $\text{C}_4$ ), 164.0 ( $\text{C}_7$ ), 157.4 ( $\text{C}_5$ ), 154.7 ( $\text{C}_9$ ), 148.2 ( $\text{C}_4'$ ), 146.1 ( $\text{C}_2$ ), 141.3 ( $\text{C}_3'$ ), 135.2 ( $\text{C}_3$ ), 125.9 ( $\text{C}_6'$ ), 121.8 ( $\text{C}_1'$ ), 115.6 ( $\text{C}_5'$ ), 112.2 ( $\text{C}_2'$ ), 101.2 ( $\text{C}_{10}$ ), 95.7 ( $\text{C}_{6,8}$ ) ppm (see Fig. 1a for carbon labelling of quercetin).

### 2.3.2. $\gamma$ -CD-Quercetin (1:1)

A solution of 200 mg of  $\gamma$ -CD (0.14 mmol) in 30 mL of water: ethanol (1:2), at ambient temperature, was added stepwise with solid quercetin (42 mg, 0.14 mmol). After full dissolution, the solution was stirred for 2 h, snap-frozen and freeze-dried to obtain a pale yellow solid in quasi-quantitative yield.

Anal. Calc. for  $(\text{C}_{48}\text{H}_{80}\text{O}_{40})(\text{C}_{15}\text{H}_{10}\text{O}_7) \cdot 16(\text{H}_2\text{O})$  (1886.6): C, 40.07; H, 6.517%; Found: C, 39.46; H, 6.178%. Thermogravimetric analysis up to 115 °C shows a mass loss of 16.2%, corresponding to the evaporation of 17 water molecules.

FT-IR (KBr,  $\text{cm}^{-1}$ ):  $\nu(\text{tilde}) = 3388\text{vs}$ , 2928m, 1657m, 1630m, 1602m, 1566m, 1518m, 1446m, 1416m, 1374m, 1324m, 1250m; 1200m, 1159s, 1126sh, 1102s, 1080s, 1052s, 1026vs, 1002sh, 942m, 936sh, 860m, 843m, 815m, 760m, 706m, 668w, 638w, 605m, 583m, 529m, 479w, 446w, 413w, 362w, 290vw, 283w.

Raman:  $\nu(\text{tilde}) = 1564\text{w}$ , 1606vs, 1590m, 1567m, 1548m, 1441s, 1401s, 1371m, 1318s, 1267w, 1217w, 1175w, 1112m, 1084w, 995w, 942w, 843w, 784w, 721w, 707w, 687w, 659w, 638m, 602s, 575m, 518m, 479s, 442w, 401w, 355w, 331w, 228w, 200w.

$^{13}\text{C}\{^1\text{H}\}$  CP/MAS NMR: 174.7 (guest,  $\text{C}_4$ ), 164.3, 163.2 (guest,  $\text{C}_7$ ), 160.2 (guest,  $\text{C}_5$ ), 156.4 (guest,  $\text{C}_9$ ), 146.9, 146.0 (guest,  $\text{C}_4'$ ), 144.9, 144.1 (guest,  $\text{C}_2$ ), 143.5 (guest,  $\text{C}_3'$ ), 134.6 (guest,  $\text{C}_3$ ), 121.6 (guest,  $\text{C}_1'$ ), 120.0 (guest,  $\text{C}_6'$ ), 115.0 (guest,  $\text{C}_5' + \gamma$ ), 103.1 ( $\gamma$ -CD,  $\text{C}_1$ ), 97.5 (guest,  $\text{C}_6$ ), 95.0 (guest,  $\text{C}_8$ ), 81.5 ( $\gamma$ -CD,  $\text{C}_4$ ), 72.8 ( $\gamma$ -CD,  $\text{C}_{2,3,5}$ ), 60.2 ( $\gamma$ -CD,  $\text{C}_6$ ).

## 2.4. Inhibition of lipid peroxidation in buffered egg yolk – TBARS assay

The anti-peroxidation evaluation followed an adaptation of the TBARS assay (Daker et al., 2007). The method relies on

the colorimetric monitoring of the malondialdehyde formed by polyunsaturated lipids degradation by reactive oxygen species (Pryor and Stanley, 1975). Treating malondialdehyde with thiobarbituric acid (TBA) produces a coloured compound. Chicken egg yolk, with a high content in lecithin, is used as a cost-effective source of unsaturated lipids.

Three independent assays were conducted for each sample. The reaction mixture contained 1 ml chicken egg yolk emulsified with 0.1 M phosphate buffer to obtain a final concentration of 0.1 g/ml, 100  $\mu$ l of 0.12 M 2,2'-azobis(2-amidinopropane) dihydrochloride (AAPH, an accelerant of the radical formation reactions), and 100  $\mu$ l of the test sample. Stock solutions (6 mL each) of 300 mg/ml of quercetin, in ethanol at 96% (v/v), and 1.2 g/ml of both  $\beta$ -CD-quercetin and  $\gamma$ -CD-quercetin, both in ethanol 70% (v/v), were prepared and diluted in each assay to obtain final sample concentrations ranging between 0.1 mM and 1.0 mM. The mixture was incubated at 37 °C for 1 h, treated with 500  $\mu$ l of freshly prepared 15% (v/v) TCA and 1.0 ml of 1% (v/v) TBA and it was kept at 95 °C for 10 min. Upon cooling, the tubes were centrifuged at 3500 rpm for 10 min to remove precipitated protein and the absorbance of the supernatant was measured at 532 nm. The control comprised buffered egg with ethanol and AAPH. The percentage of inhibition of peroxidation was calculated using a simple formula (1)

$$\%_{\text{inhibition}} = \frac{A_0 - A_s}{A_0} \times 100 \quad (1)$$

where  $A_0$  is the absorbance of the control and  $A_s$  is the absorbance of the sample.

### 2.5. Anti-oxidant capacity by the DPPH method

The antiradical activities were measured against the coloured free radical 2,2-diphenyl-1-picrylhydrazyl (DPPH $\cdot$ ) (Brand-Williams et al., 1995). A methanol stock solution of DPPH $\cdot$  (15.0 mL) was prepared to have Abs<sub>515nm</sub> within 0.9–1.0 (in our experimental conditions this was achieved with 500  $\mu$ M). Three independent assays were carried out for each sample. In a 96-well plate, 0.1 mL of sample is mixed with 0.1 mL diluted DPPH $\cdot$ . Seven dilutions were tested: 0.5–40  $\mu$ M for pure quercetin and 10–100  $\mu$ M for the inclusion compounds (which have lower activity). DPPH $\cdot$  bleaching was followed at 515 nm at 0 min, 5 min, and every 5 min until steady state is reached (20 min under our experimental conditions). The EC<sub>50</sub> is the sample concentration causing, at the steady state, 50% reduction of the DPPH $\cdot$  initial concentration.

**Antiradical efficacy.** The antioxidant/radical action determined by the DPPH assay is best expressed as antiradical efficiency (AE) (Sanchez-Moreno et al., 1998). This parameter is evaluated by using, for each sample, a solution with a concentration equal to its EC<sub>50</sub> value. A mixture of 0.1 mL of the test sample and 0.1 mL of DPPH $\cdot$  (500  $\mu$ M) and the Abs<sub>510nm</sub> is read at 0 min, 2 min, and every 2 min until reaching 50% discoloration (the Abs<sub>510nm</sub> is half of the value at time zero). At this time point, the test compound is expressing 50% of antioxidant activity, and it is thus deemed t<sub>EC50</sub>. The antiradical efficacy (AE) is calculated using the formula (2):

$$AE = \frac{1}{EC_{50} \times t_{EC50}} \quad (2)$$

### 2.6. Incorporation of $\beta$ -CD-quercetin and $\gamma$ -CD-quercetin into fresh cheese

Bovine raw milk was pasteurised at 74 °C for 30 s. After cooling to 34 °C, it was added with powdered milk (40.0 g L<sup>-1</sup>), sodium chloride (9.0 g L<sup>-1</sup>), calcium chloride solution (0.7 mg L<sup>-1</sup>) and animal rennet (0.035 g L<sup>-1</sup>), comprising roughly 90% of chymosin and pepsin. The mixture rested at 32–33 °C for 15–20 min to allow the curd to be formed. The curd was then roughly cut to start the whey release process, drained under rest for 5 min and kneaded to further remove whey and other liquids. The incorporation of the inclusion compounds was carried out after this step. Finally, the curd mass was divided, placed into individual fresh cheese moulds and stored in the refrigerator until its consumption. The final concentrations in the fresh cheese were 0.029% (m/m) for  $\beta$ -CD-quercetin and 0.043% (m/m) for  $\gamma$ -CD-quercetin, values that are fully safe for human ingestion.

### 2.7. Sensory analysis

To evaluate possible changes in the organoleptic characteristics of the cheeses resulting from the addition of the inclusion compounds, a sensory analysis was conducted using a Product Preference Test on a panel of 30 non-trained tasters. This test evaluates the preference of a given product by a consumer. Samples of non-treated fresh cheese and fortified fresh cheese were presented randomly to each panellist for them to state their preference for one of the samples and issue a small comment about the products. The results were treated by the Pearson's chi-squared test.

## 3. Results and discussion

### 3.1. Preparation of the inclusion compounds

Inclusion of quercetin into  $\beta$ -CD and  $\gamma$ -CD was carried out by co-dissolution procedures. For food applications, and given the good aqueous solubility of CDs, water is the elected solvent. Quercetin has low water solubility and low wettability, thus needing ethanol to dissolve. The two solutions are mixed to obtain a clear co-solution where CD and quercetin interact to form complexes. The solutions are then subject to snap-freezing and the frozen solvent is removed by lyophilisation. The initial host: guest molar ratio was 1:1, and elemental analysis result that this stoichiometry was maintained in the isolated solid products.

### 3.2. Solid-state characterisation of the inclusion compounds

The freeze-dried solids were studied by a range of techniques to confirm quercetin inclusion and to evaluate the purity and stability of the compounds and study the geometry of inclusion of quercetin into each CD and the supramolecular packing of the complex units in the solid state.

#### 3.2.1. Vibrational spectroscopy

Quercetin possesses several functional groups which are likely to suffer shifts by encapsulation. The carbonyl stretching band,  $\nu(\text{C}=\text{O})$ , is particularly well-observed in Fourier



**Table 1** Selected FT-IR bands for quercetin and its  $\beta$ - and  $\gamma$ -CD inclusion compounds.

Selected bands ( $\text{cm}^{-1}$ )			Approximate description <sup>a</sup>
Quercetin	$\beta$ -CD-quercetin	$\gamma$ -CD-quercetin	
1664	1660	1657	$\nu(\text{C}=\text{O})$
1612	1612	1630, 1600	$\nu(\text{C}=\text{C})_{\text{ring C}}$
1560	1560	1566	$\nu(\text{C}=\text{C})_{\text{ring B (mode 8a')}}^b$
1522	1522	1517	$\nu(\text{C}=\text{C})_{\text{rings A, B}}$
1319	1324	1324	$\nu(\text{C5}-\text{OH})$
1261	1263	1250	$\nu(\text{C}=\text{C})_{\text{ring B (mode 14)}}, \nu(\text{O1}-\text{C2}), \nu(\text{C3}-\text{O3}), \nu(\text{C3}-\text{C4}), \nu(\text{C4}-\text{C10})^b$

<sup>a</sup> (Briggs and Colebrook, 1962; Cornard et al., 1997).

<sup>b</sup> The description of the stretching modes for the substituted benzene ring (B) follows Wilson's notation (Wilson, 1934).

Transform infrared spectroscopy (FT-IR). It appears at relatively low frequency ( $1664 \text{ cm}^{-1}$ ) which, in early investigations, was attributed to an intramolecular  $\text{C5}-\text{O}-\text{H} \cdots \text{O}=\text{C}$  hydrogen bond (Fig. 1b), referred to as a “conjugate-chelate” type (Briggs and Colebrook, 1962). The bond would, however, be quite strong, implying a  $\nu(\text{C}-\text{O})$  frequency even lower than the one observed. A more realistic model was recently presented. Structural studies of solid anhydrous quercetin using a combination of molecular modelling, PXRD and solid-state NMR data (Filip et al., 2013) have proposed that in solid quercetin there is a network of intra- and intermolecular hydrogen bonds, with a more homogeneous charge distribution and lower C—O polarisation (Fig. 1c).

After inclusion into the CDs the  $\nu(\text{C}-\text{O})$  band of quercetin suffers a shift, as well as other quercetin bands. These changes are listed in Table 1. Note how the spectrum  $\gamma$ -CD-quercetin presents several shifted guest bands. These bands are associated with stretching modes of guest aromatic rings, thus suggesting that the entire quercetin molecule is included into the wide cavity of  $\gamma$ -CD. In comparison, the host-guest interaction occurring in  $\beta$ -CD-quercetin appears to be weaker, as only two oscillators present shifts. The C—O stretch is redshifted by  $-4 \text{ cm}^{-1}$  and the C5—OH stretch is blueshifted by  $+5 \text{ cm}^{-1}$ . These changes suggest the disruption of the network hydrogen bonds found in pure quercetin and to the formation of a new hydrogen bond with  $\beta$ -CD, most likely at the secondary hydroxyls located at its larger rim of this macrocycle, lowering the  $\nu(\text{C}-\text{O})$  frequency due to the increased degree of polarisation. The interaction of quercetin with  $\beta$ -CD is thus postulated to occur superficially, at the larger rim, instead of involving inclusion of quercetin into the cavity. This proposed interaction model is coherent with previous  $^1\text{H}$  NMR studies in solution which show partial inclusion of quercetin into  $\beta$ -CD (Zheng et al., 2004), and also with the solid-state  $^{13}\text{C}\{^1\text{H}\}$  CP-MAS NMR data herein presented (Section 3.2.3).

The Raman spectrum of  $\gamma$ -CD-quercetin further confirms the inclusion. The carbonyl stretch occurs at  $1654 \text{ cm}^{-1}$ , redshifted by  $-6 \text{ cm}^{-1}$  in comparison with pure quercetin; other bands are blueshifted by c.a.  $+2 \text{ cm}^{-1}$ , namely the C—C bands of rings B and A, found at  $1548$  and  $1441 \text{ cm}^{-1}$  for  $\gamma$ -CD-quercetin and at  $1546$  and  $1439 \text{ cm}^{-1}$ , respectively, for pure quercetin.

### 3.2.2. Powder X-ray diffraction and morphology

The diffraction pattern for freeze-dried  $\gamma$ -CD-quercetin (Fig. 2) shows a quasi-amorphous material that crystallises as a new phase upon rehydration by storing the solid for a few hours

in a vapour-saturated chamber. Note that this phase (Fig. 2d) is free from reflections of pure quercetin or  $\gamma$ -CD heptahydrate, evidencing that  $\gamma$ -CD-quercetin is a true and pure inclusion compound (Caira, 2001). Its stability against disruption by moisture demonstrates strong host-guest affinity. To further demonstrate the stability, the inclusion constant of  $\gamma$ -CD-quercetin was determined (see details in section S3 of the Electronic Supplementary information), having a value of  $K_{app} = 1805.4 \text{ M}^{-1}$ .

The diffraction pattern of the hydrated sample of  $\gamma$ -CD-quercetin provides information on the cyclodextrin packing mode. Note that the pattern shares good similarities with that of  $\gamma$ -CD-12-crown-4-ether (Kamitori et al., 1986), a model compound in which the units of inclusion complex are stacking to form channels (Fig. 3). According to isostructurality principle of CD inclusion compounds reported by Caira (Caira, 2001) such similarity implies that the  $\gamma$ -CD-quercetin complex units are also channel-packed.

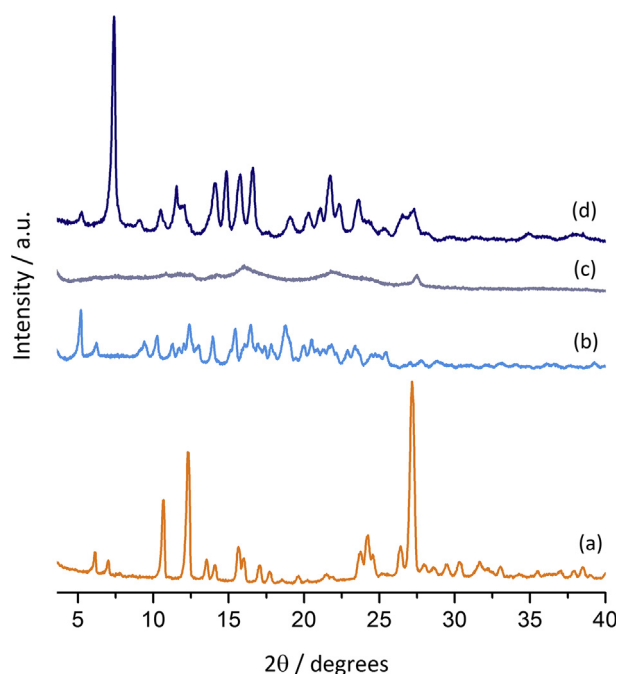


**Figure 2** Experimental powder X-ray diffraction patterns of (a) quercetin, (b)  $\gamma$ -CD heptahydrate, (c) the freeze-dried  $\gamma$ -CD-quercetin product (obtained in an amorphous form) and (d) the same product after rehydration (in a vapour-saturated chamber).

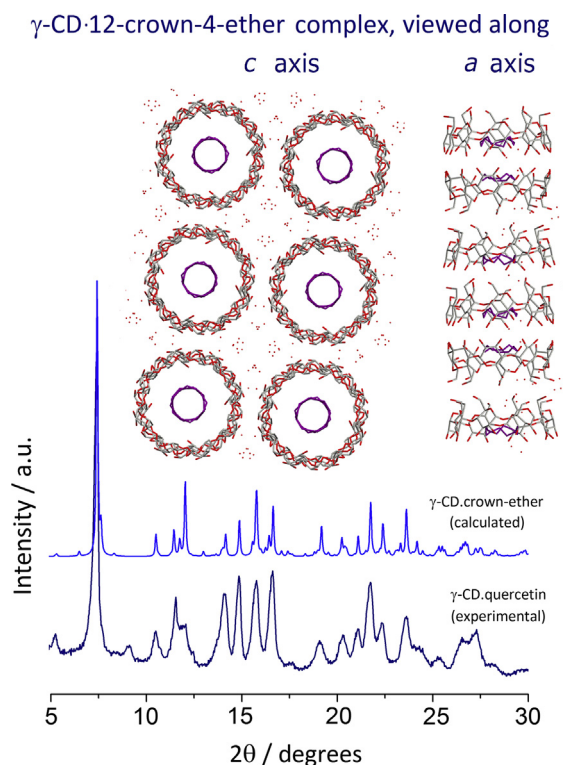


**Figure 3** Comparison of the experimental powder diffraction pattern of the rehydrated sample of  $\gamma$ -CD-quercetin with that of a model inclusion complex,  $\gamma$ -CD-12-crown-4-ether. The trace of the model compound was calculated using the software Mercury (v3.5.1, ©CCDC 2001–2014) on the atomic coordinates of  $\gamma$ -CD-12-crown-4-ether (Kamitori et al., 1986). Structural details of this model complex are depicted above the diffractogram, with the guest highlighted in purple colour.

Freeze-dried  $\beta$ -CD-quercetin is a fully amorphous material, which, upon rehydration, evidences recrystallisation of a small portion of  $\beta$ -CD and quercetin, indicative of low host-guest affinity (Fig. S1 in the Electronic Supplementary Information). The inclusion constant ( $K_{app}$ ) values for  $\beta$ -CD-quercetin, obtained from phase solubility studies, varies between  $402 \text{ M}^{-1}$  (Pralhad and Rajendrakumar, 2004) and  $602 \text{ M}^{-1}$  (Jullian et al., 2007), indicating a mild affinity. This means that water molecules in the saturated chamber are able to displace some of the quercetin molecules out of the  $\beta$ -CD cavities, leading these to re-crystallise as pure quercetin.

The powdered samples of pure quercetin,  $\gamma$ -CD heptahydrate (as-received from the manufacturer) and rehydrated  $\gamma$ -CD-quercetin were studied by scanning electron microscopy (SEM) to evaluate the following: i) crystal morphology, ii) crystal integrity, and iii) material homogeneity. Quercetin is entirely composed of very small needle-shaped crystals (Fig. 4b and e). The pure  $\gamma$ -CD host presents a good number of fragments of crystals and some particles with the rough shape of parallelepipeds albeit with rounded edges and multiple cracking on the surface (Fig. 4a and d). Given the high solubility of this cyclodextrin in water, the fragmentation and cracking are likely to reflect a fast drying method employed by the manufacturer to obtain it quickly and in a good yield. Regarding the inclusion compound, it is possible to observe

the formation of microcrystals with plate-like shape throughout the bulk material (Fig. 4c and f). This morphology is coherent with the observations made by powder X-ray diffraction that evidence a new crystalline phase for this inclusion compound.

### 3.2.3. $^{13}\text{C}\{^1\text{H}\}$ CP-MAS spectroscopy

The solid-state  $^{13}\text{C}\{^1\text{H}\}$  CP-MAS spectra of  $\gamma$ -CD-quercetin, pure quercetin and  $\gamma$ -CD are depicted in Fig. 5. Note how the resonances ascribed to the host present multiple signals in the case of pure  $\gamma$ -CD and appear as single signals in the spectrum of the inclusion compound, indicating that the ring of  $\gamma$ -CD has adopted a more symmetric conformation to present a larger cavity, able to accommodate quercetin better.

The resonances ascribed to the guest, quercetin, also feature relevant changes in the spectrum of  $\gamma$ -CD-quercetin, as listed in Table 2. The signals ascribed to the carbons 2' and 5' of the catechol (B ring) are superimposed while other carbons are presenting two or multiple resonances, namely C2, C4', C7' and the carbons 6 + 8, which give rise to a single resonance in pure quercetin. This indicates an overall change in the chemical environment around these molecules and the occurrence of two or more different geometries of inclusion (Braga et al., 2002).

In the spectrum of  $\beta$ -CD-quercetin, the resonances of both the host and the guest carbons appear mostly unchanged in comparison with those observed in the spectra of pure quercetin and  $\beta$ -CD hydrate (see Table 2 and Fig. S2 in the Electronic Supplementary Information). This indicates a weak host-guest interaction and further confirms that quercetin is located outside the cavity of  $\beta$ -CD, rather interacting with its rim as postulated from FT-IR data.

### 3.2.4. Thermogravimetry

Thermal decomposition profiles for the pure CDs, quercetin,  $\beta$ -CD-quercetin,  $\gamma$ -CD-quercetin and their 1:1 physical mixtures (PMs) were collected and compared (Figs. 6 and 7).

The TG traces of the pure hosts,  $\beta$ -CD (Fig. 6) and  $\gamma$ -CD (Fig. 7), are characterised by an initial dehydration step, which starts at ambient temperature and proceeds up to  $75^\circ\text{C}$  for  $\beta$ -CD and to  $95^\circ\text{C}$  for  $\gamma$ -CD. Both CDs have a mass loss from dehydration of 15%, that translates into 11 hydration waters for  $\beta$ -CD and 12 for  $\gamma$ -CD. Quercetin dehydrates between  $65$  and  $135^\circ\text{C}$ , having no further mass loss until  $290^\circ\text{C}$ , which marks the onset of its thermal oxidation (Da Costa et al., 2002; Masek and Chrzescijanska, 2015). From  $360^\circ\text{C}$  onwards, there is a second and steeper degradation step and, at  $515^\circ\text{C}$ , all quercetin is decomposed. The steps associated with quercetin's oxidative and thermal degradation are absent in both the PMs and the adducts, evidencing the interaction of quercetin with the CDs. Decomposition of the host occurs around  $250^\circ\text{C}$  for  $\beta$ -CD-quercetin and its PM, and at  $270^\circ\text{C}$  for  $\gamma$ -CD-quercetin and its PM. The traces of the inclusion compounds differ from those of PMs only in the dehydration process which takes place in two separate steps in the PMs (CD and quercetin waters have different evaporation temperatures). In  $\gamma$ -CD-quercetin, mass loss from dehydration is 16%, corresponding to 17 water molecules, in good consonance with microanalysis and being higher than the water content of the PM and of pure  $\gamma$ -CD. The stacking of  $\gamma$ -CD molecules into channels (shown in PXRD), in turn arranged into squares,

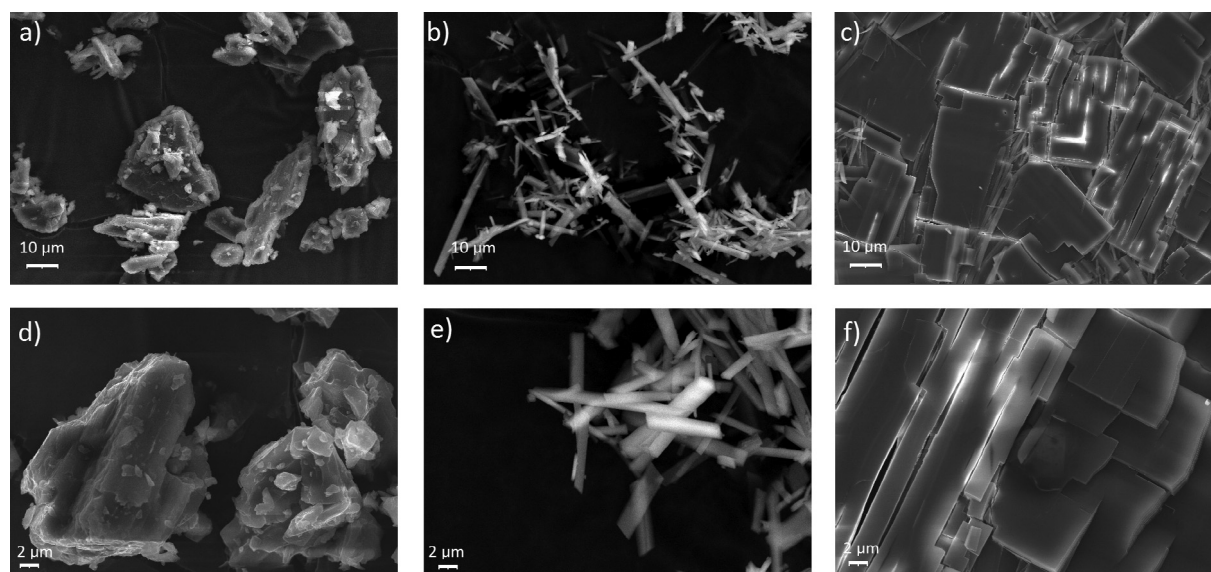


**Figure 4** SEM images of  $\gamma$ -CD (a and d), quercetin (b and e) and rehydrated  $\gamma$ -CD-quercetin (c and f) at two different magnifications: the images on the top line of the figure show a broader view at low magnification (scale bar represents 10  $\mu\text{m}$ ) and the images on the bottom line show the same samples with a higher magnification (scale bar represents 2  $\mu\text{m}$ ) for a more detailed view of the morphology.

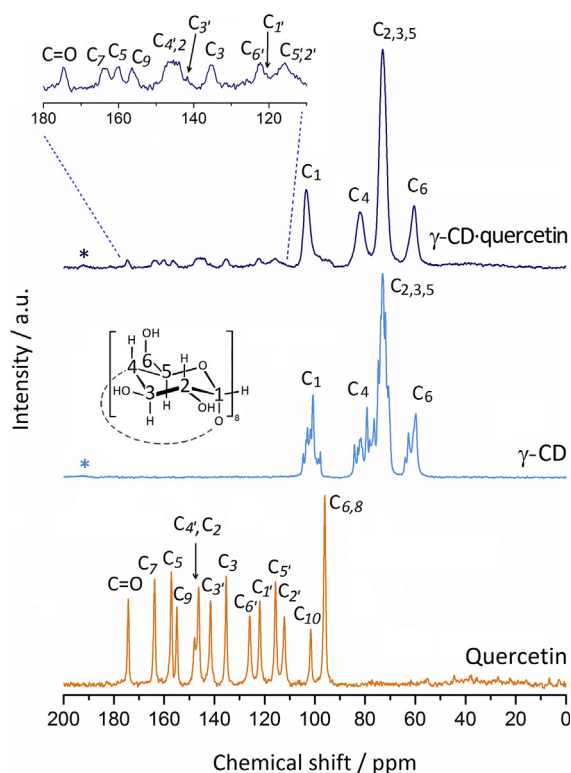


**Figure 5** Solid-state  $^{13}\text{C}\{^1\text{H}\}$  CP-MAS spectra of  $\gamma$ -CD-quercetin,  $\gamma$ -CD and pure quercetin. Spinning side bands are marked with asterisks.

**Table 2**  $^{13}\text{C}\{^1\text{H}\}$  CP-MAS NMR resonances of quercetin and its 1:1 adducts with  $\beta$ - and  $\gamma$ -cyclodextrins.

Quercetin	$\beta$ -CD-Quercetin	$\gamma$ -CD-Quercetin	Assignment
174.4	174.1	174.7	Guest, $\text{C}_4$
164.0	163.8	164.3, 163.2	Guest, $\text{C}_7$
157.4	157.2	160.2	Guest, $\text{C}_5$
154.7	154.6	156.4	Guest, $\text{C}_9$
148.2	147.9	146.9, 146.0	Guest, $\text{C}_{4'}$
146.1	146.2	144.9, 144.1	Guest, $\text{C}_2$
141.3	141.5	143.5	Guest, $\text{C}_{3'}$
135.2	135.1	134.6	Guest, $\text{C}_3$
125.9	125.9	121.6	Guest, $\text{C}_{6'}$
121.8	122.0	120.0	Guest, $\text{C}_{1'}$
115.6	115.5	115.0	Guest, $\text{C}_{5'}$
112.2	112.1	115.0	Guest, $\text{C}_{2'}$
—	104.2, 103.3, 102.2, 101.4	103.1	$\beta$ - or $\gamma$ -CD, $\text{C}_1$
101.2	<i>n.o.</i>	<i>n.o.</i>	Guest, $\text{C}_{10}$
95.7	95.9	97.5	Guest, $\text{C}_6$
95.7	95.9	95.0	Guest, $\text{C}_8$
—	84.2, 83.3, 82.3, 81.2, 80.4, 78.4	81.5	$\beta$ - or $\gamma$ -CD, $\text{C}_4$
—	76.3, 75.2, 73.8, 73.0, 72.6, 71.6	72.8	$\beta$ - or $\gamma$ -CD, $\text{C}_{2,3,5}$
—	63.7, 62.2, 60.3, 59.6, 58.7	60.2	$\beta$ - or $\gamma$ -CD, $\text{C}_6$

Notes: *n.o.* means the signal was not observed due to overlapping with signals of the cyclodextrin host.

Assignment of quercetin carbon resonances was based on both its  $^{13}\text{C}$  spectrum dms $\text{-d}_6$  solution (Lalleman & Duteil, 1977) and on the calculated chemical shifts for solid quercetin (Filip et al., 2013).

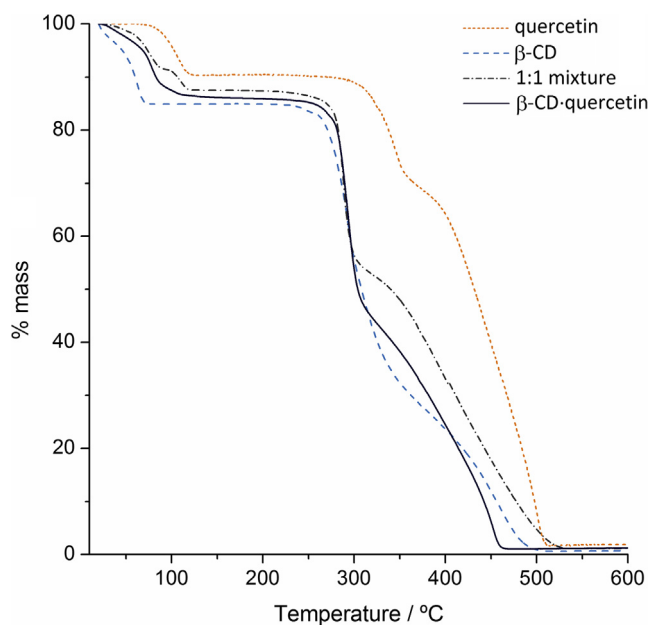


**Figure 6** TG traces for  $\beta$ -CD, quercetin,  $\beta$ -CD-quercetin and the 1:1 physical mixture of  $\beta$ -CD and quercetin.

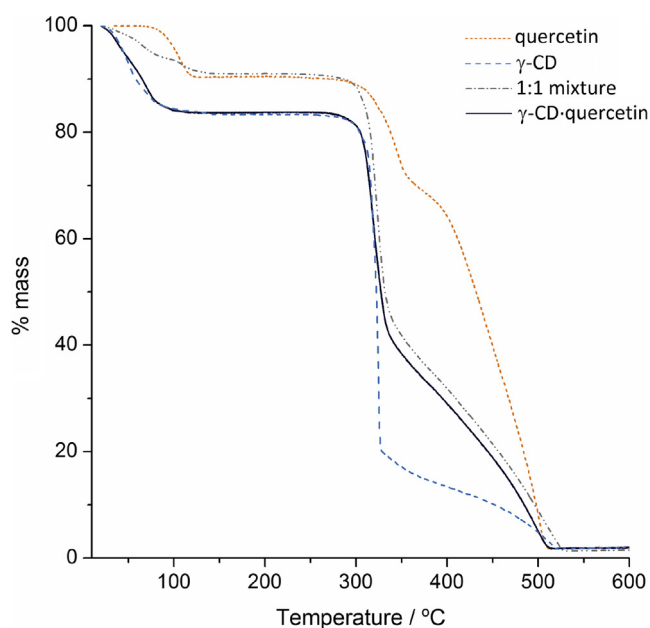


**Figure 7** TG traces for  $\gamma$ -CD, quercetin,  $\gamma$ -CD-quercetin and the 1:1 physical mixture of  $\gamma$ -CD and quercetin.

leaves wide inter-channel spaces suitable to accommodate a large number of water molecules (Fig. 3, inset).

### 3.3. Antioxidant activity studies

Cyclodextrin inclusion is reported to improve the activity of some guests, namely concerning their antioxidant action (Castrejn et al., 1997). CDs are known to modulate the antioxidant activity of flavones, caffeic acid, tea catechins and astaxanthin (Aree and Jongrungruangchok, 2016; Folch-Cano

et al., 2010; García-Padial et al., 2013; Lucas-Abellán et al., 2008; Mercader-Ros et al., 2010; Sueishi et al., 2012).

#### 3.3.1. Evaluation of the lipid peroxidation inhibition with the TBARS assay

Lipid peroxidation, by accumulation of reactive oxygen species (ROS) such as the superoxide anion, hydroxyl radicals, nitric oxide and the peroxy radical, is an important mechanism of food deterioration (Antolovich et al., 2002). The TBARS assay is an indirect measure of a compounds' ability to block ROS and a good first approach to gather evidence on their capability to interfere with oxidation processes occurring in food matrices (Fig. 8a).

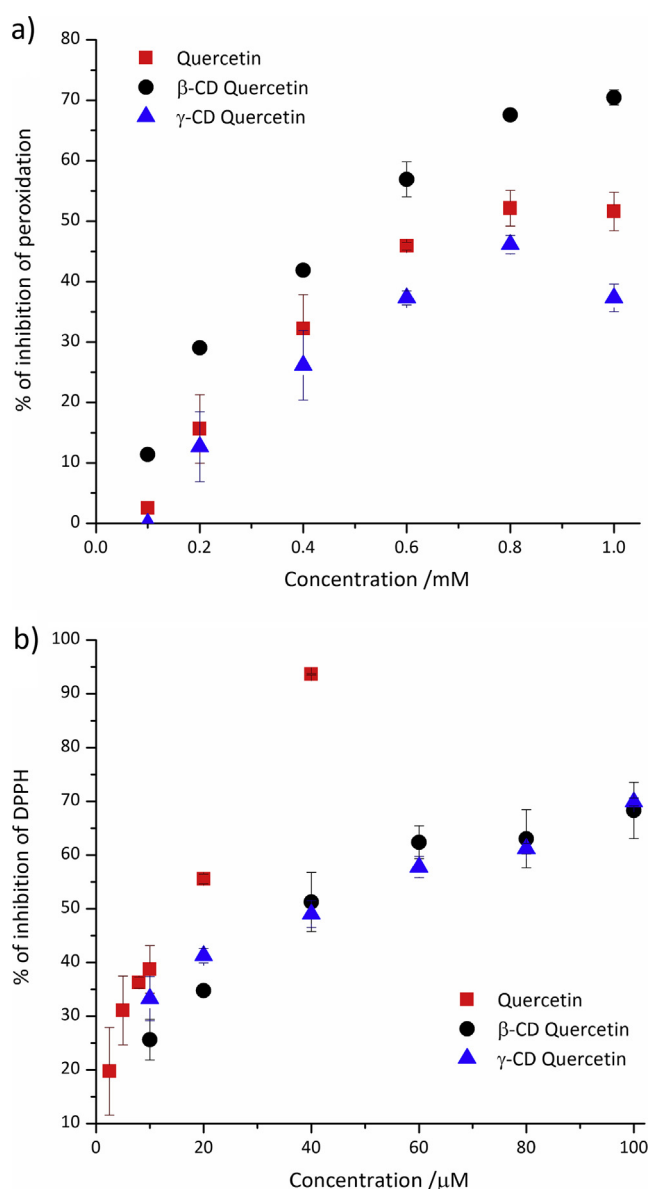


**Figure 8** Antioxidant action of  $\gamma$ -CD-quercetin, compared with pure quercetin and  $\beta$ -CD-quercetin. (a) Results of the lipid peroxidation assay using buffered egg yolk; (b) results of the DPPH scavenging assay, measured at 20 min of incubation. Data points represent the mean  $\pm$  SD of three independent assays.



$\beta$ -CD-quercetin displayed the highest percentage of inhibition, followed by quercetin and  $\gamma$ -CD-quercetin. The activity is quasi dose-dependent; that is, it increases with the concentration, up to 0.8 mM. At higher concentration, the activity of  $\beta$ -CD-quercetin continues to increase but not in a dose-dependent mode, while the activities of quercetin and  $\gamma$ -CD-quercetin start to decrease, possibly due to occurrence of a pro-oxidant mechanism at a high concentration. The different behaviour of  $\beta$ -CD-quercetin may result from the fact that quercetin is more readily available in this adduct since it is not located in the host cavity. In addition, quercetin can dissociate easily (as demonstrated by powder diffraction after contact with moisture), being able to act freely while having higher solubility in the reaction medium due to the presence of  $\beta$ -CD.

### 3.3.2. Evaluation of radical scavenging properties with the DPPH assay

In this assay the test compound scavenges the free radical DPPH $\cdot$ , causing the test solution to change colour and thus allowing the reaction progress to be easily monitored by UV-Vis spectroscopy (refer to Section S2 of the ESI for details). The percentage of unreacted DPPH $\cdot$  at different concentrations of quercetin or inclusion compounds is given in Fig. 8b. The EC<sub>50</sub> is determined by simple interpolation.

The t<sub>EC50</sub> and the antiradical efficiency (AE) are presented in Table 3. These parameters can be determined by measuring the kinetics of inhibition using the concentration which corresponds to the EC<sub>50</sub> of the test compound (calculation details given in the Experimental Section).

Quercetin is a very efficient radical scavenger even at low concentrations. At concentrations above 40  $\mu$ M, the activity reaches a plateau (not shown) and, overtime, quercetin may eventually begin to act as a pro-oxidant. The inclusion compounds present very similar DPPH $\cdot$  scavenging curve profiles,

both requiring high concentrations to exhibit radical scavenging action. The kinetics of reaction is, however, faster, as 50% of the DPPH $\cdot$  is bleached in roughly one third of the time required with quercetin. The antiradical efficacy values (AE), weighing these two previous factors, are thus slightly higher for the inclusion compounds, particularly for  $\beta$ -CD-quercetin.

### 3.4. Incorporation of CD-quercetin inclusion compounds into fresh cheese

The incorporation of the inclusion compounds into the cheese curd was carried out after the whey was drained, to avoid possible bleaching during this process. The mass was roughly homogenised, divided into moulds and stored in the refrigerator (Fig. 9).

#### 3.4.1. Sensory evaluation

Fortification of fresh cheese with CD-quercetin, even in a low percentage (0.03–0.04% of mass), produced minor changes in its organoleptic characteristics, particularly in the colour and texture. Fortified fresh cheese was more compact and less “watery”, likely owing to the ability of cyclodextrins to retain water molecules and to improve the texture and flavour of low fat products (Reineccius et al., 2004). Fortified fresh cheese presented a yellow colour and a “dotted” aspect, particularly with  $\gamma$ -CD-quercetin.

In the product preference test (refer to Table S1 for details), fortified and untreated fresh cheeses scored very similar, with *p*-values of 0.3 for  $\beta$ -CD-quercetin, and 0.4 for  $\gamma$ -CD-quercetin. These values, calculated for one degree of freedom (fortified *vs* non-treated), are far above the limit of statistically significant difference (*p* < 0.05) thus meaning that the incorporation of CD-quercetin does not cause significant differences to the acceptance of fresh cheese by tasters.

#### 3.4.2. Shelf-life assessment of fresh cheese fortified with CD-quercetin adducts

To evaluate the stability over the time of storage, the pH of untreated and fortified fresh cheese samples was monitored once a week over three weeks (refer to Table S2 of the electronic supplementary Information for the list of measured pH values). After one week of storage, non-treated samples presented pH values around 5.5 and the fortified ones had pH around 5.7. After the second week, however, all the cheese samples had pH > 5, evidencing a degradation

**Table 3** Parameters of radical scavenging activity (with DPPH $\cdot$ ) for quercetin and its  $\beta$ - and  $\gamma$ -CD inclusion compounds.

Compound	EC <sub>50</sub> / $\mu$ M	t <sub>EC50</sub> /min	AE $\times 10^3$ / $\mu$ M <sup>-1</sup> min <sup>-1</sup>
Quercetin	17	54	1.09
$\beta$ -CD-quercetin	50	14	1.43
$\gamma$ -CD-quercetin	50	16	1.25



**Figure 9** Incorporation of  $\beta$ -CD-quercetin into the cheese curd (left) and division of the curd mass into individual moulds (right).

process most likely caused by fermentation of residual lactose to lactic acid by either pasteurisation-resistant indigenous bacteria in milk or post-production contamination with environmental bacteria. It can thus be concluded that the shelf-life of fresh cheese is not altered by the fortification with CD-quercetin adduct.

#### 4. Conclusions

The present work clearly demonstrated that  $\gamma$ -cyclodextrin is the most suitable host to form a stable inclusion compound with quercetin in the solid state. The co-dissolution/freeze-drying method was shown to afford this adduct in a 1:1 host-guest molar stoichiometry and with quasi-quantitative. Solid-state characterisation has shown that quercetin is deeply included into the cavity of  $\gamma$ -CD, as a result of the wide diameter of this host's cavity. We were also able to propose a channel packing mode for  $\gamma$ -CD-quercetin and to demonstrate its stability against disruption by moisture. In turn, the narrower cavity  $\beta$ -CD makes it less suitable for the inclusion of quercetin in the solid state and interaction occurs only at the rim of this host.

The strong host-guest interaction in  $\gamma$ -CD-quercetin has implications on its anti-lipidic peroxidation activity, as demonstrated by the TBARS assay. Included quercetin is less active, probably due to its lower ability to interact with the substrate in this matrix. Regarding the DPPH $\cdot$  scavenging ability, cyclodextrin inclusion led to a faster onset of action (reaction kinetics roughly three times faster than with pure quercetin), but activity was observed at higher concentrations.

Inclusion compounds are readily incorporated into fresh cheese during the curd stage. At the concentrations tested (0.03–0.04% mass), fortified fresh cheese exhibited only minor organoleptic alterations, namely a firmer texture and a yellowish colour. These differences do not affect its overall perception and acceptance, given that the product preference test has revealed no statistical difference between treated and non-treated fresh cheese. The process herein described is thus a practical way to prepare fresh cheese with nutraceutical properties which can be easily adapted to large-scale production, and the product is expected to be well accepted by the consumers.

#### Acknowledgments

The supply of  $\beta$ -CD and  $\gamma$ -CD (pharmaceutical grade Cava-max W7 and W8, respectively, manufactured by Wacker-Chemie) by Ashland Specialty Ingredients (Düsseldorf, Germany) is gracefully acknowledged. We are also grateful to Fundação para a Ciência e a Tecnologia (FCT, Portugal), European Union, QREN, European Fund for Regional Development (FEDER), through the programme COMPETE, for general funding to the QOPNA research unit (project Pest C-QUI/UI0062/2013; FCOMP-01-0124-FEDER-037296).

A very special thanks is owed to Marta Ferro for assisting with collecting the SEM images and also to David Gomes, M<sup>a</sup> Adélia Vaz and M<sup>a</sup> Lurdes Pires for assisting in the manufacture of fresh cheese and in the incorporation of the CD-quercetin adducts into fresh cheese.

#### Appendix A. Supplementary material

Supplementary data associated with this article can be found, in the online version, at <http://dx.doi.org/10.1016/j.arabjc.2017.04.001>.

#### References

- Antolovich, M., Prenzler, P.D., Patsalides, E., McDonald, S., Robards, K., 2002. Methods for testing antioxidant activity. *Analyst* 127, 183–198.
- Aree, T., Jongrungruangchok, S., 2016. Crystallographic evidence for  $\beta$ -cyclodextrin inclusion complexation facilitating the improvement of antioxidant activity of tea(+)catechin and (–)-epicatechin. *Carbohydr. Polym.* 140, 362–373.
- Bae, H.Y., Kim, S.Y., Kwak, H.S., 2008. Comparison of cholesterol-reduced Camembert cheese using crosslinked beta-cyclodextrin to regular Camembert cheese during storage. *Milchwissenschaft* 63, 153–156.
- Bae, H.Y., Kim, S.Y., Ahn, S.Y., Kwak, H.S., 2009. Properties of cholesterol-reduced Feta cheese made by crosslinked beta-cyclodextrin. *Milchwissenschaft* 64, 165–168.
- Bergonzi, M.C., Bilia, A.R., Di Bari, L., Mazzi, G., Vincieri, F.F., 2007. Studies on the interactions between some flavonols and cyclodextrins. *Bioorg. Med. Chem. Lett.* 17, 5744–5748.
- Boots, A.W., Haenen, G.R.M.M., Bast, A., 2008. Health effects of quercetin: from antioxidant to nutraceutical. *Eur. J. Pharmacol.* 585, 325–337.
- Braga, S.S., Aree, T., Imamura, K., Vertut, P., Boal-Palheiros, B., Saenger, W., et al., 2002. Structure of the  $\beta$ -cyclodextrin p-hydroxybenzaldehyde inclusion complex in aqueous solution and in the crystalline state. *J. Incl. Phenom. Macro.* 43, 359–366.
- Brand-Williams, W., Cuvelier, M.E., Berset, C., 1995. Use of the free radical method to evaluate antioxidant activity. *Lebensm.-Wiss. Technol.* 28, 25–30.
- Briggs, L.H., Colebrook, L.D., 1962. Infra-red spectra of flavanones and flavones. Carbonyl and hydroxyl stretching and CH out-of-plane bending absorption. *Spectrochim. Acta* 18, 939–957.
- Caira, M.R., 2001. On the isostructurality of inclusion complexes and its practical utility. *Rev. Roum. Chim.* 46, 371–386.
- Castrejón, S.E., Yatsimirsky, A.K., La, S., 1997. Cyclodextrin enhanced fluorimetric determination of malonaldehyde by the thiobarbituric acid method. *Talanta* 44, 951–957.
- Cornard, J.P., Merlin, J.C., Boudet, A.C., Vrielynck, L., 1997. Structural study of quercetin by vibrational and electronic spectroscopies combined with semiempirical calculations. *Biospectroscopy* 3, 183–193.
- Da Costa, E.M., Barbosa Filho, J.M., Do Nascimento, T.G., Macêdo, R.O., 2002. Thermal characterization of the quercetin and rutin flavonoids. *Thermochim. Acta* 392–393, 79–84.
- Daker, M., Abdullah, N., Vikineswary, S., Goh, P., Kuppusamy, U., 2007. Antioxidant from maize and maize fermented by *Marasmiellus* sp. as stabiliser of lipid-rich foods. *Food Chem.* 107, 1092–1098.
- Filip, X., Grosu, I.-G., Miclăuş, M., Filip, C., 2013. NMR crystallography methods to probe complex hydrogen bonding networks: application to structure elucidation of anhydrous quercetin. *CrystEngComm* 15, 4131–4142.
- Folch-Cano, C., Jullian, C., Speisky, H., Olea-Azar, C., 2010. Antioxidant activity of inclusion complexes of tea catechins with  $\beta$ -cyclodextrins by ORAC assays. *Food Res. Int.* 43, 2039–2044.
- García-Padial, M., Martínez-Ohárriz, M.C., Navarro-Blasco, I., Zornoza, A., 2013. The role of cyclodextrins in ORAC-fluorescence assays. antioxidant capacity of tyrosol and caffeic acid with hydroxypropyl- $\beta$ -cyclodextrin. *J. Agric. Food Chem.* 61, 12260–12264.
- Hollman, P.C., Gaag, M., Mengelers, M.J., van Trijp, J.M., de Vries, J.H., Katan, M.B., 1996. Absorption and disposition kinetics of the dietary antioxidant quercetin in man. *Free Radical Biol. Med.* 21 (5), 703–707.
- Hollman, P.C., van Trijp, J.M., Mengelers, M.J., de Vries, J.H., Katan, M.B., 1997a. Bioavailability of the dietary antioxidant flavonol quercetin in man. *Cancer Lett.* 114 (1–2), 139–140.

- Hollman, P.C., van Trijp, J.M., Buysman, M.N., van der Gaag, M.S., Mengelers, M.J., de Vries, J.H., et al, 1997b. Relative bioavailability of the antioxidant flavonoid quercetin from various foods in man. *FEBS Lett.* 418 (1–2), 152–156.
- Jullian, C., Moyano, L., Yañez, C., Olea-Azar, C., 2007. Complexation of quercetin with three kinds of cyclodextrins: an antioxidant study. *Spectrochim. Acta A* 67, 230–234.
- Jung, H.J., Ganesan, P., Lee, S.J., Kwak, H.S., 2013. Comparative study of flavor in cholesterol removed Gouda cheese and Gouda cheese during ripening. *J. Dairy Sci.* 96, 1972–1983.
- Kamitori, S., Hirotsu, K., Higuchi, T., 1986. Crystal and molecular structure of the  $\gamma$ -cyclodextrin–12-crown-4 1:1 inclusion complex. *J. Chem. Soc., Chem. Commun.*, 690–691.
- Koontz, J.L., Marcy, J.E., O’Keefe, S.F., Duncan, S.E., 2009. Cyclodextrin inclusion complex formation and solid-state characterization of the natural antioxidants  $\alpha$ -tocopherol and quercetin. *J. Agric. Food Chem.* 57, 1162–1171.
- Kozłowska, A., Szostak-węgierek, D., 2014. Flavonoids – food sources and health benefits. *Rocz. Panstw. Zakł. Hig.* 65, 79–85.
- Lallemand, J.Y., Duteil, M., 1977.  $^{13}\text{C}$  n.m.r. spectra of quercetin and rutin. *Org. Magnet. Res.* 9 (3), 179–180.
- Lanilai.com, 2016. Lanilai relaxation drinks. <<http://lanilai.com/anti-stress-drink-benefits/>> (accessed 6 October 2016).
- Lucas-Abellán, C., Mercader-Ros, M.T., Zafrilla, M.P., Fortea, M.I., Gabaldón, J.A.A., Núñez-Delgado, E., 2008. ORAC-Fluorescein assay to determine the oxygen radical absorbance capacity of resveratrol complexed in cyclodextrins. *J. Agric. Food Chem.* 56, 2254–2259.
- Marcolino, V.A., Zanin, G.M., Durrant, L.R., Benassi, M.D.T., Mاتيoli, G., 2011. Interaction of curcumin and bixin with  $\beta$ -cyclodextrin: complexation methods, stability, and applications in food. *J. Agric. Food Chem.* 59, 3348–3357.
- Masek, A., Chrzescijanska, E., 2015. Effect of UV-A irradiation and temperature on the antioxidant activity of quercetin studied using ABTS, DPPH and electrochemistry methods. *Int. J. Electrochem. Sci.* 10, 5276–5290.
- Mercader-Ros, M.T., Lucas-Abellán, C., Fortea, M.I., Gabaldón, J.A., Núñez-Delgado, E., 2010. Effect of HP- $\beta$ -cyclodextrins complexation on the antioxidant activity of flavonols. *Food Chem.* 118, 769–773.
- Paul, P., Bhattacharyya, S., 2015. Antioxidant profile and sensory evaluation of cookies fortified with juice and peel powder of fresh Pomegranate (*Punica granatum*). *Int. J. Agric. Food Sci.* 5 (3), 89–91.
- Pereira, A.B., Braga, S.S., 2015. Cyclodextrin Inclusion of Nutraceuticals, from the Bench to your Table. In: Ramirez, F.G. (Ed.), *Cyclodextrins: Synthesis, Chemical Applications and Role in Drug Delivery*, Novascience Publishers, Hauppauge, New York, pp. 195–224.
- Pralhad, T., Rajendrakumar, K., 2004. Study of freeze-dried quercetin–cyclodextrin binary systems by DSC, FT-IR, X-ray diffraction and SEM analysis. *J. Pharm. Biomed. Anal.* 34, 333–339.
- Pryor, W.A., Stanley, J.P., 1975. Suggested mechanism for the production of malonaldehyde during the autoxidation of polyunsaturated fatty acids. Nonenzymic production of prostaglandin endoperoxides during autoxidation. *J. Org. Chem.* 40, 3615–3617.
- Quercetin.com, 2016. Quercetin Food Chart. <<http://www.quercetin.com/overview/food-chart>> (accessed 29 March 2016).
- Ramírez-Ambrosi, M., Caldera, F., Trotta, F., Berrueta, L.A., Gallo, B., 2014. Encapsulation of apple polyphenols in  $\beta$ -CD nanosponges. *J. Incl. Phenom. Macrocycl. Chem.* 80, 85–92.
- Rasaie, S., Ghanbarzadeh, S., Mohammadi, M., Hamishehkar, H., 2014. Nano phytosomes of quercetin: a promising formulation for fortification of food products with antioxidants. *Pharm. Sci.* 20, 96–101.
- Reineccius, T.A., Reineccius, G.A., Peppard, T.L., 2004. Potential for  $\beta$ -cyclodextrin as partial fat replacer in low-fat foods. *J. Food Sci.* 69 (FCT334–FCT341).
- Rothe, J., Wakileh, M., Dreissiger, K., Weber, H., 2015. The flavonoid beverage Haelan 951 induces growth arrest and apoptosis in pancreatic carcinoma cell lines in vitro. *BMC Complement. Altern. Med.* 212 (13 pages).
- Sanchez-Moreno, C., Larrauri, J.A., Saura-Calixto, F., 1998. A procedure to measure the antiradical efficiency of polyphenols. *J. Sci. Food Agric.* 76, 270–276.
- Sen, G., Mukhopadhyay, S., Ray, M., Biswas, T., 2008. Quercetin interferes with iron metabolism in *Leishmania donovani* and targets ribonucleotide reductase to exert leishmanicidal activity. *J. Antimicrob. Chemother.* 61, 1066–1075.
- Senthilkumar, K., Elumalai, P., Arunkumar, R., Banudevi, S., Gunadharini, N.D., Sharmila, G., Selvakumar, K., Arunakaran, J., 2010. Quercetin regulates insulin like growth factor signaling and induces intrinsic and extrinsic pathway mediated apoptosis in androgen independent prostate cancer cells (PC-3). *Mol. Cell. Biochem.* 344, 173–184.
- Stobiecki, M., Kachlicki, P., 2006. Isolation and identification of flavonoids. In: Grotewold, E. (Ed.), *The Science of Flavonoids*. Springer, New York, pp. 47–69.
- Sueishi, Y., Ishikawa, M., Yoshioka, D., Endoh, N., Oowada, S., Shimmei, M., Fujii, H., Kotake, Y., 2012. Oxygen radical absorbance capacity (ORAC) of cyclodextrin-solubilized flavonoids, resveratrol and astaxanthin as measured with the ORAC-EPR method. *J. Clin. Biochem. Nutr.* 50, 127–132.
- Tahir, M.N., Kwon, C., Jeong, D., Cho, E., Paik, S.R., Jung, S., 2013. *J. Dairy Sci.* 96, 4191–4196.
- Thilakarathna, S.H., Rupasinghe, H.P.V., 2013. Flavonoid bioavailability and attempts for bioavailability enhancement. *Nutrients* 5, 3367–3387.
- Yehuda, N.B., Anglea, T.A., 2010. Flavonoid-rich citrus extract process. US Patent 20100159115 A1 (December 19th).
- Young, O.A., Gupta, R.B., Sadooghy-Saraby, S., 2012. Effects of cyclodextrins on the flavor of goat milk and its yogurt. *J. Food Sci.* 77, S122–S127.
- Wilson, E.B., 1934. The normal modes and frequencies of vibration of the regular plane hexagon model of the benzene molecule. *Phys. Rev.* 45, 706–714.
- Zheng, Y., Haworth, I.S., Zuo, Z., Chow, M.S.S., Chow, A.H.L., 2004. Physicochemical and structural characterization of quercetin– $\beta$ -cyclodextrin complexes. *J. Pharm. Sci.* 94 (5), 1079–1089.